

1

2 **1 Title:** A strongly improved assembly of the pearl millet reference genome using Oxford
3 Nanopore long reads and optical mapping

4

5 **4 Authors:**

6 Marine Salson¹, Julie Orjuela¹, Cédric Mariac¹, Leïla Zekraoui¹, Marie Couderc¹, Sandrine
7 Arribat², Nathalie Rodde², Adama Faye^{3,4}, Ndjido A. Kane^{3,4}, Christine Tranchant-Dubreuil¹,
8 Yves Vigouroux^{1§}, Cécile Berthouly-Salazar^{1§}

9

10 **9 Affiliation :**

11 10 ¹DIADE, Université de Montpellier, Institut de Recherche pour le Développement,
12 Montpellier, France

13 12 ²Centre National de Ressources Génomiques Végétales (CNRGV), Institut national de
14 recherche pour l'agriculture, l'alimentation et l'environnement (INRAE), Castanet Tolosan,
15 France

16 15 ³Centre d'Etude Régional pour l'Amélioration de l'Adaptation à la sécheresse (CERAAS),
17 ISRA Thiès, Sénégal

18 17 ⁴LAPSE: Laboratoire Mixte International Adaptation des Plantes et microorganismes
19 associés aux Stress Environnementaux (LMI LAPSE), Dakar, Sénégal

20

21 20 [§]These authors contributed equally: Yves Vigouroux* and Cécile Berthouly-Salazar*

22 *Corresponding author. Tel: +33467416,439.

23 22 E-mail address: yves.vigouroux@ird.fr; cecile.berthouly@ird.fr.

24

25

26 26 **Keywords:** pearl millet, assembly, Oxford Nanopore long reads, optical mapping

2

27 **Abstract**

28

29 Pearl millet (*Pennisetum glaucum* (L.)) R. Br. syn. *Cenchrus americanus* (L.) Morrone) is an important
30 crop in South Asia and sub-Saharan Africa which contributes to ensure food security. Its genome has
31 an estimated size of 1.76 Gb and displays a high level of repetitiveness above 80%. A first assembly
32 was previously obtained for the Tift 23D2B1-P1-P5 cultivar genotype using short-read sequencing
33 technologies. This assembly is however incomplete and fragmented with around 200 Mb unplaced on
34 chromosomes. We report here an improved quality assembly of the pearl millet Tift 23D2B1-P1-P5
35 cultivar genotype obtained with an approach combining Oxford Nanopore long reads and Bionano
36 Genomics optical maps. This strategy allowed us to add around 200 Mb at the chromosome-level
37 assembly. Moreover we strongly improved continuity in the order of the contigs and scaffolds within
38 the chromosomes, particularly in the centromeric regions. Notably, we added more than 100 Mb
39 around the centromeric region on chromosome 7. This new assembly also displayed a higher gene
40 completeness with a complete BUSCO score of 98.4% using the Poales database. This more complete
41 and higher quality assembly of the Tift 23D2B1-P1-P5 genotype now available to the community will
42 help in the development of research on the role of structural variants, and more broadly in genomics
43 studies and the breeding of pearl millet.

3

44 Introduction

45

46 Pearl millet (*Pennisetum glaucum* (L.) R. Br. syn. *Cenchrus americanus* (L.) Morrone) is a cereal
47 adapted to high temperature and is mainly cultivated in sub-Saharan Africa and South Asia. It is the
48 staple food for more than 90 million farmers, and research projects aiming to improve this crop's
49 productivity and resilience may thus contribute to greater food security. Obtaining a more complete
50 pearl millet reference genome assembly and improving its quality will help us to better carry out
51 genetic and genomic studies of this important crop.

52

53 Next generation sequencing technologies such as Illumina technology enabled the acquisition of a
54 large number of genomes in the 2010s, including non-model species both in the animal and plant
55 kingdoms. A genome for pearl millet was assembled and published in 2017 (Varshney et al. 2017)
56 using the inbred Tift 23D2B1-P1-P5 cultivar genotype as the reference (BioSample identifier:
57 SAMN04124419). Pearl millet is a cross-pollinated diploid with 7 chromosomes ($2n = 14$). Its genome
58 size was estimated at 1.76 Gb with more than 80% repetitive sequences (Varshney et al. 2017).
59 However around 200 Mb remained unplaced in the pearl millet reference genome (Varshney et al.
60 2017) and the chromosomes were fragmented and displayed a high Ns content above 13%
61 (GCA_002174835, European Nucleotide Archive).

62

63 Assembly of large and complex genomes obtained with short-read sequencing technologies are often
64 incomplete and fragmented (Belser et al. 2018). Combining long-read sequencing and optical
65 mapping has proven to be an effective approach to improve the quality of assemblies of complex plant
66 genomes over the last few years (Belser et al. 2018, Istace et al. 2021, Belser et al. 2021, Aury et al.
67 2022). Recent studies performed with genomes of higher quality have highlighted the importance of
68 structural variations such as inversions in the evolution and adaptation of species (Wellenreuther and
69 Bernatchez 2018, Huang and Rieserberg 2020,). A high-quality reference genome is, however,
70 required to detect and study such variants. To improve the quality of the Tift 23D2B1-P1-P5 genome,
71 we therefore generated Bionano Genomics optical maps and long reads obtained by Oxford
72 Nanopore Technologies (ONT) sequencing. The combined use of these two types of data allowed us
73 to improve the N50 of scaffolds by 100 fold with a N50 of 86 Mb, and we added around 200 Mb at the
74 chromosome-level assembly. The improvement of the quality of the assembly was also verified by
75 comparing the chromosomes of both the new and the previous genomes with the optical maps
76 obtained for a control line PMiGAP257/IP-4927. The comparison highlighted the better continuity in
77 the order of the contigs and the scaffolds of the new assembly, notably in the centromeric regions.
78 This assembly will thus allow more efficient identification of structural variants in pearl millet
79 populations and a better understanding of the genomics of this important crop.

4

80 Material and methods

81

82 *Plant materials and Sequencing*

83 Biological material for both accessions was obtained from ICRISAT in Niamey. For Tift 23D2B1-P1-
84 P5, genotyping of 14 SSRs was used to ensure the homozygosity of the individual extracted.
85 PMiGAP257/IP-4927 is an inbred line from a Senegalese souna pearl millet.

86 High molecular weight DNA extraction was performed using a previous published protocol (Mariac et
87 al. 2019). Briefly, the isolation of plant nuclei is performed from 1 gram of young fresh leaves
88 previously ground in liquid nitrogen. The isolated nuclei are then lysed (MATAB) and the DNA purified
89 with chloroform/isoamyl alcohol (24:1) and then precipitated with isopropanol. All transfer steps were
90 performed with a pipette tip cut at the extremity and homogenization steps were performed by slow
91 inversion to limit mechanical shearing of the DNA molecules. DNAs were quantified by fluorometry
92 (Qubit) and qualitatively assessed using pulsed field electrophoresis to ensure that fragment sizes
93 ranged from 40-150 kb. Oxford Nanopore DNA library preparation (SQKLSK109-PromethION,
94 Genomic DNA ligation protocol) and sequencing were performed by Novogen Co., LTD.

95

96 *Long-read ONT Assembly and polishing*

97 The different steps of the assembly are summarized in Figure S1.

98 Base calling on Oxford Nanopore Technologies (ONT) reads was performed with guppy (v. 6.0.6, and
99 the dna_r9.4.1_450bps_hac_prom.cfg model). Reads shorter than 5 kb and with a quality score below
100 10 were excluded with NanoFilt (v. 1.0, De Coster et al. 2018).

101 The ONT assembly was performed with filtered reads using the CulebrONT pipeline (Orjuela et al.
102 2022, v 2.1.0) and Flye assembler (v. 2.9, Kolmogorov et al. 2019). Two rounds of Racon (v. 1.5.0,
103 Vaser et al. 2017) and Medaka (v. 1.6.1, <https://github.com/nanoporetech/medaka>) were also used to
104 polish and correct the contigs using the ONT reads. The ONT contigs were finally polished with high
105 quality Illumina short reads using Hapo-G (v 1.3, Aury and Istace 2021). The short reads from the
106 same Tift 23D2B1-P1-P5 genotype (175 Gb of raw data corresponding to 97X coverage, NCBI SRA
107 accession SRP063925, Varshney et al. 2017) were trimmed with cutadapt (v3.1, -m 35, -q 30.30
108 parameters, Martin 2011) and aligned to the ONT contigs using bwa-mem2 (v 2.2.1, Vasimuddin et al.
109 2019) with -l 210,100,500,100 parameters to handle two different insert sizes in the short reads
110 paired-end libraries of 170 and 250 bases. Only properly paired reads were kept using the software
111 samtools (v. 1.9, -f 0x02 parameter, Danecek et al. 2021) and two rounds of short reads correction
112 with Hapo-G (v 1.3, Aury and Istace 2021) were performed with default parameters (Aury and
113 Istace 2021).

114 Purge Haplotigs (Roach et al. 2018) was used in order to identify potential false duplications in the
115 assembly. The long reads were aligned to the ONT contigs with minimap2 (v. 2.24, Li H. 2018) and
116 the hist command of Purge Haplotigs (v. 1.1.1, Roach et al. 2018) was launched to obtain an
117 assembly-wide read depth histogram.

118 ***Optical mapping data generation and comparison with current pearl millet reference genome***

119 Ultra-HMV DNA extraction and optical map generation was carried out using the Bionano Prep Plant
120 tissue DNA Isolation and Bionano Prep Direct Label and Stain Label (DLS) protocols, and was
121 performed by the French Plant Genomic Resources Centre (CNRGV) of the French National
122 Research Institute for Agriculture, Food and Environment (INRAE). Optical mapping data were
123 generated for the Tift 23D2B1-P1-P5 and the PMiGAP257/IP-4927 genotypes with Bionano Genomics
124 Saphyr system. The DLE-1 enzyme and the Direct Label and Stain technology were used. Molecules
125 smaller than 150 kb and with less than 9 labels were excluded. *De novo* assembly was performed
126 with the filtered molecules using Bionano Solve pipeline (v. 3.5.1, Shelton et al. 2015).

127 The 7 chromosomes of the pearl millet reference genome (Varshney et al. 2017, GCA_002174835.1)
128 were converted into optical maps using the *fa2cmap_multi_color.pl* script of Bionano Solve (v3.3,
129 Shelton et al. 2015) and were aligned with the Tift 23D2B1-P1-P5 assembled optical maps using the
130 *runCharacterize.py* script of Bionano Solve with RefAligner and the default parameters (v3.3, Shelton
131 et al. 2015, Yuan et al. 2020). Alignments were visualized with Bionano Access (v 3.7, Yuan et al.
132 2020) and the cumulative size of the optical maps assigned to each chromosome was calculated. The
133 optical maps were assigned to the chromosome with which they shared the longest aligned region.
134 We calculated the Pearson correlation coefficient between the reference chromosome lengths and the
135 cumulative sizes of the optical maps aligned to each chromosome with the R function *cor.test()* (R
136 version 4.2.1) and visually inspected the correlation using the function *geom_smooth()* of the R
137 package *ggplot2* (v. 3.3.6, Wickham H 2016).

138

139 ***Hybrid Scaffolding with Optical Maps***

140 Hybrid scaffolding was performed with both the ONT contigs and the assembled optical maps of the
141 Tift 23D2B1-P1-P5 genotype using Bionano Solve (v. 3.3, *hybridScaffold.pl* script with -B 2 -N 2
142 parameters, Shelton et al. 2015). We then used the Bionano Scaffolding Correction Tool (BiSCoT v.
143 2.3.3, Istace et al. 2020) with the default parameters in order to remove artefactual duplications from
144 the hybrid scaffolds. TGS Gap-Closer (v. 1.2.0, Mengyang Xu et al. 2020) was used to perform gap
145 filling and reduce the total number of Ns in the hybrid scaffolds. This step may also correct the lack of
146 Bionano precision in predicting the size of gaps below 10 kb (Mengyang Xu et al. 2020). We only
147 used ONT reads with a quality score Q > 12 and length greater than 10 kb. Additionally, we corrected
148 these ONT long reads using Illumina high quality short reads with Hapo-G (v 1.3, Aury and
149 Istace 2021). TGS Gap-Closer (v. 1.2.0, Mengyang Xu et al. 2020) was run using these corrected
150 ONT reads with more stringent criteria than the default parameters by requiring at least two reads to
151 bridge a gap. We then performed a last step of high quality short reads correction of the hybrid
152 scaffolds with Hapo-G (v 1.3, Aury and Istace 2021).

153 Purge Haplotigs (v. 1.1.1, Roach et al. 2018) was then used again to detect some potential false
154 duplications in the hybrid scaffolds.

155 ***Building Chromosome Scale Assembly and Structure validation***

156 We used the RagTag tool (Alonge et al. 2019) with the pearl millet reference genome as a guide
157 (Varshney et al. 2017, GCA_002174835.1) in order to regroup the hybrid scaffolds and construct the 7
158 chromosomes. We launched RagTag (v. 2.1.0, Alonge et al. 2019) with the default parameters in
159 order to obtain grouping, location and orientation confidence scores for each scaffold.

160 However, due to potential assembly errors in the genome used as a guide, we applied more stringent
161 criteria than the default parameters and we only kept scaffolds with a grouping confidence score
162 above 0.7. An in depth study, along with manual curation, was performed for one very large scaffold
163 of 68 Mb with a grouping confidence score under 0.7. This scaffold displayed regions of tens of Mb in
164 length aligned to two chromosomes and was identified as chimeric. It was manually cut in conformity
165 with the alignments performed with minimap2 (v. 2.4, Li H. 2018) and visualized with D-genies (v. 1.4,
166 Cabanettes F. and Klopp C. 2018) interactive dot plots on the two chromosomes.

167 In addition, we performed visual controls to check the position and the orientation of the scaffolds
168 within each chromosome. We aligned the new chromosomes constructed with RagTag with the
169 optical maps of another inbred genotype PMiGAP257/IP-4927 which served as a control. Optical map
170 alignments to the new chromosomes were performed with the *runCharacterize.py* script of Bionano
171 Solve using RefAligner and the default parameters (v. 3.3, Shelton et al. 2015, Yuan et al. 2020) and
172 were visualized with Bionano Access (v. 3.7, Yuan et al. 2020). If necessary, we used reverse
173 complement sequence and manually moved some scaffolds based on abnormalities observed in
174 alignments (Table S1).

175 To compare the new and previously obtained genome sequences, alignments were made between
176 the chromosomes of the two assemblies using minimap2 (v. 2.24, Li H. 2018) and D-genies (v. 1.4,
177 Cabanettes F. and Klopp C. 2018) in order to visualize alignments: we enabled the “hide noises”
178 option and only plotted alignments with more than 50% identity. We also compared optical map
179 alignments of the PMiGAP257/IP-4927 line between the new and the old assemblies (Varshney et al.
180 2017), to assess the improvement of the structure in the new assembly. We did not use optical maps
181 of Tift 23D2B1-P1-P5 because since they were used for hybrid scaffolding, they showed perfect
182 alignments with the new assembly.

183 ***Transposable Element Detection, Gene Completeness estimation and Annotation, and***
184 ***Centromere Localization***

185 A *de novo* transposable elements (TEs) library was generated from the pearl millet reference genome
186 (Varshney et al. 2017) with RepeatModeler2 (v. 2.0.1, options -engine NCBI, Flynn et al. 2020). TEs
187 were then detected on the new assembly using RepeatMasker (v. 4.1.2, Tarailo-Graovac and
188 Chen 2009) with the *de novo* TEs library.

189 The gene completeness of the new assembly was estimated with BUSCO (v. 5.4.3, Manni et al. 2021)
190 and the Poales dataset (odb10) composed of 4896 genes.

191 Annotation of the new genome was performed with Liftoff (v 1.6.3, Shumate et al. 2020) using the
192 annotation files of the Tift 23D2B1-P1-P5 reference genome available at
193 <http://dx.doi.org/10.5524/100192> (Varshney et al. 2017). The genes were aligned to the new assembly
194 with minimap2 (v2.24, Li H. 2018) and were considered correctly mapped if a minimum of 50% of the
195 genes were aligned to the new assembly and with a sequence identity higer than 50% (-s 0.5 -a 0.5
196 parameters). We also enabled annotation of gene copies using a minimum identity threshold of 95% (-
197 copies -sc 0.95 parameters).

198 We localized the centromeric regions on chromosomes with a satellite sequence of 137 bp specific to
199 the pearl millet centromere (GenBank accession: Z23007.1, Kamm et al. 1994). We used BLAST (v.
200 2.9.0+, Altschul et al. 1990) to align and determine the positions of the centromeric specific sequence
201 on the chromosomes of the new assembly. We only kept alignments longer than 100 bases with
202 shared identities higher than 80%. We also aligned this satellite sequence to the hybrid scaffolds in
203 order to further validate their orientation and positions during the building of the chromosome scale
204 assembly.

8

205 Results and discussion

206

207 *Optical Map Assembly and Comparison of Tift 23D2B1-P1-P5 with current pearl millet* 208 *reference genome*

209 A total of 1,806 Gb of data were generated for the Tift 23D2B1-P1-P5 genotype. After excluding
210 molecules shorter than 150 kb and with fewer than 9 labels, a total of 574 Gb of data remained with
211 an N50 of 219 kb corresponding to 383X coverage of the estimated size of the pearl millet genome.
212 Assembly of the filtered molecules led to 164 optical maps with a total length of 1.99 Gb and a
213 length N50 of 44.8 Mb.

214 A total of 90 optical maps were aligned to the reference genome, representing a total size of 1.94 Gb
215 with a N50 of 45.2 Mb. The remaining 74 unaligned optical maps have a N50 20 times shorter with
216 2.2 Mb, and represented 52 Mb.

217 The correlation between the cumulative lengths of the optical maps assigned to each chromosome
218 and the chromosome sizes of the reference genome was marginally significant (Pearson correlation
219 coefficient $r=0.54$, $p\text{-value}=0.059$). Chromosome 7 was indeed an outlier as optical maps aligned to
220 this chromosome were 128 Mb larger than expected (Figure S2). When removing chromosome 7, the
221 correlation for the six other chromosomes was high and significant (Pearson correlation coefficient
222 $r=0.90$, $p\text{-value}=0.015$).

223 Optical map alignments can help to identify mis-assembly (Yuan et al. 2020). We highlighted several
224 cases of misalignments between the Tift 23D2B1-P1-P5 optical maps and the pearl millet
225 chromosomes (Figures S3), suggesting some potential assembly errors in the pearl millet reference
226 genome. These misalignments are especially observed around the centromeric regions (Table S2), as
227 expected due to the difficulties in assembling them (Belser et al. 2018).

228

229 Concerning the PMiGAP257/IP-4927 genotype, a total of 2,586 Gb of data were generated. After
230 excluding molecules shorter than 150 kb and with fewer than 9 labels, a total of 685 Gb of data
231 remained with an N50 of 213 kb corresponding to 403X coverage of the estimated pearl millet
232 genome. Assembly of the filtered molecules led to 346 assembled optical maps with a total length of
233 2.48 Gb and a N50 length of 25.2 Mb.

234

235 *Long Reads ONT Assembly and Hybrid Scaffolding*

236 A total of 6,261,759 ONT reads from the Tift 23D2B1-P1-P5 genotype were generated with a
237 cumulative size of 108 Gb, corresponding to a mean depth of 60X.

238 For the assembly, we only kept reads with a quality score higher than 10 and larger than 5 kb. A total
239 of 2,640,214 long reads remained, with a read length N50 of 25.2 kb and a mean size of 21.8 kb after
240 quality filtering. The total sequence data amount used for the assembly was 57.6 Gb, corresponding
241 to a mean depth of 32X for this inbred genotyped.

242 Assembly with Flye and polishing led to 3,641 ONT contigs with a N50 of 1.2 Mb. The N50 length of
243 the contigs is 67 times longer than the contigs N50 obtained from the previous Tift 23D2B1-P1-P5
244 genome (Table 1, Varshney et al. 2017).

9

245 Hybrid scaffolding of ONT contigs using the Bionano optical maps led to 72 hybrid scaffolds with a
246 cumulative length of 1.86 Gb. The N50 length of these scaffolds is 86 Mb, which is roughly 100 times
247 greater than the previous assembly (Table 1, Varshney et al. 2017). The total length of the remaining
248 1,161 unplaced ONT contigs represented 55 Mb with a N50 of 68 kb. We finalized this hybrid
249 scaffolding by bridging gaps with TGS Gap-Closer, leading to a strong decrease in N bases from
250 4.31% to 0.29%.

251

252 ***Reference Guided Chromosome Construction***

253 Of the 72 hybrid scaffolds, 53 displayed a grouping confidence score above 0.7 to a single
254 chromosome using RagTag. One scaffold showed ~ 42 Mb aligned to chromosome 5 and ~ 26 Mb
255 aligned to chromosome 4 and was therefore identified as chimeric and manually split (Table S1:
256 Scaffold_8135). The two split scaffolds then showed high grouping confidence scores (Table S1).

257 We also manually reversed the sequence of a scaffold of 88 Mb assigned to chromosome 3 with low
258 orientation confidence score (Table S1: Scaffold_1980). Alignments of the centromeric repetitive
259 sequence were found both at the beginning of Scaffold_1980 and at the beginning of the following
260 scaffold (Table S1: Scaffold_3136), which supported the decision to reverse Scaffold_1980.
261 Orientation of this large scaffold was confirmed when comparing the new assembly both with the
262 optical maps of the control line PMiGAP257/IP-4927 and with the chromosome 3 of the previous
263 reference genome (Figure 1).

264 Two other large scaffolds of 147 and 105 Mb also displayed good but below 0.7 grouping confidence
265 scores to chromosome 7 (Table S1: Scaffold_1301 and Scaffold_2567). These two large scaffolds led
266 to a new chromosome 7 around 105 Mb larger than chromosome 7 of the reference genome
267 (Varshney et al. 2017), in accordance with the inference made previously with the optical maps
268 (Figure S2). In addition, centromere specific sequence repeats were identified at the extremities of
269 these two large scaffolds positioned one after another and further supported their positions and their
270 orientations. Because we also discarded the possibility of major duplications in the new assembly
271 using Purge haplotigs analysis (Figure S4), we hypothesized that the centromeric region of the
272 chromosome 7 was previously not well assembled in the reference genome and assigned these two
273 scaffolds to the new chromosome 7. This was validated by subsequent analyses presented in the next
274 section.

275

276 The total length of the new final assembly was 1.85 Gb and the cumulative size of the chromosomes
277 was 1.78 Gb. This is very close to the pearl millet estimated genome size (1.76 Gb, Varshney et al.
278 2017). We assembled 96% of the genome on chromosomes compared to 87% in the previous
279 Tift 23D2B1-P1-P5 assembly (Varshney et al. 2017) which corresponds to more than 200 additional
280 Mb at the chromosome-level assembly. Chromosomes also displayed very low Ns content (0.29%)
281 compared to the chromosomes of the previous assembly (above 13%).

10

282 ***Genes Completeness and Structure Accuracy of the Assembly***

283 The percentage of complete BUSCO genes of the Poales database found in the new assembly was
284 98.4%. Only 3.3% of the BUSCO genes were duplicated genes. This figure is in accordance with that
285 expected (Guan et al. 2020). The percentage of interspersed repeats found on the chromosomes is
286 81.7%, a percentage also in accordance with previous study on the pearl millet genome (Varshney et
287 al. 2017).

288 Concerning the 38,579 gene model from the Tift 23D2B1-P1-P5 pearl millet reference genome
289 (Varshney et al. 2017), 37,814 sequences (98.0%) were mapped at least once to the new assembly
290 with a mean coverage and a mean identity of 97.5% and 96.2% respectively. A total of 36,898 genes
291 (95.6%) were found on the 7 new chromosomes. This improved the number of genes found on
292 chromosomes by 1,107 compared to the previous Tift 23D2B1-P1-P5 reference. Both the BUSCO
293 scores and mapping of genes to the new assembly revealed enhanced gene completeness in the new
294 chromosomal sequences.

295

296 A large region of more than 100 Mb was added to the chromosome 7 of the new assembly. An excess
297 of genes annotated on the unplaced scaffolds of the previous reference genome were mapped to this
298 new chromosome 7: of the 2,342 genes originating from the unplaced scaffolds of the previous
299 assembly and mapped to the new chromosomes, a total of 1,101 genes (47%) were found on the new
300 chromosome 7. This observation added weight to our longer assembly for chromosome 7.

301

302 The alignments of our new assembly with the previous Tift 23D2B1-P1-P5 reference genome showed
303 overall good matches all along the chromosomes, particularly at the extremities (Figure 1). The
304 regions around the centromeres (Table S2) showed the strongest divergence in alignments (Figure 1),
305 a pattern previously observed and expected in comparisons between long read and short read
306 assemblies (Belser et al. 2018).

307 Optical map alignments with the PMiGAP257/IP-4927 line enabled us to validate the order and the
308 orientation of the scaffolds within the new manually curated chromosomes (Figure S5). In addition,
309 PMiGAP257/IP-4927 optical map alignments with both the new and the previous assemblies helped
310 us to assess the improvement in the structure and the continuity of the new chromosomes.
311 Alignments of these optical maps to the 7 new chromosomes showed much better overall continuity
312 compared to the previous Tift 23D2B1-P1-P5 reference genome (Figure S5). The better alignments
313 are particularly noticeable in the centromeric regions (Figure S5).

314

315 **Conclusion**

316 We present here an assembly obtained with both Oxford Nanopore long reads and Bionano
317 Genomics optical maps for the pearl millet Tift 23D2B1-P1-P5 cultivar genotype. This assembly
318 displays improvement compared to the previous pearl millet reference genome (Varshney et al. 2017),
319 in terms of both continuity and gene completeness. Obtaining high quality references is important to
320 be able to study genomic diversity and structural variants in a species. This new version will thus help
321 us to better study structural variants within pearl millet populations.

11

322 **Data Availability Statement**

323 The Tift 23D2B1-P1-P5 (BioSample identifier: SAMN04124419) pearl millet reference assembly
324 (Varshey et al. 2017) is available both in the NCBI (ASM217483v1) and through the European
325 Nucleotide Archive (GCA_002174835.1). Raw Illumina short reads from Tift 23D2B1-P1-P5 genotype
326 used for assemblies and ONT long reads polishing are accessible in NCBI with SRA
327 accession SRP063925 (list of SRR identifiers used: SRR2489264-SRR2489273). Transfer annotation
328 to the new assembly was performed using the genome annotation file pearl_millet_gff.gz available at
329 <http://dx.doi.org/10.5524/100192>.

330 The new chromosome-level assembly of the Tift 23D2B1-P1-P5 genotype (GCA_947561735.1,
331 http://www.ebi.ac.uk/ena/browser/view/GCA_947561735.1) and data used for this study including the
332 ONT long reads (run accession: ERR10627707) and the Bionano optical maps (analysis accessions:
333 ERZ14864807 for PMiGAP257/IP-4927 and ERZ14865266 for Tift 23D2B1-P1-P5) have been
334 deposited in the European Nucleotide Archive under the study accession PRJEB57746. The gff file
335 resulting from the annotation transfer is also available under the analysis accession ERZ15184682.

336

337 **Acknowledgements**

338 We acknowledge James Tregear and Anne-Céline Thuillet for help in the design of the figures.
339 The authors acknowledge the ISO 9001 certified IRD i-Trop HPC (South Green Platform) at IRD
340 Montpellier for providing HPC resources that have contributed to the research results reported within
341 this report.

342

343 **Conflict of Interest**

344 The authors declare that the research was conducted in the absence of any commercial or financial
345 relationships that could be construed as a potential conflict of interest.

346

347 **Funder information**

348 This study was supported by an ANR grant (ANR-19-CE02-00006-1, PEMILADAPT project) to CB.
349 MS received a PhD scholarship from the French government.

350 Literature cited

351

352 Alonge M, Soyk S, Ramakrishnan S, Wang X, Goodwin S, Sedlazeck Fritz J., Lippman Zachary
353 B. Schatz Michael M. (2019) RaGOO: fast and accurate reference-guided scaffolding of draft
354 genomes. *Genome Biol* 20, 224. <https://doi.org/10.1186/s13059-019-1829-6>

355

356 Altschul SF, Gish W, Miller W, Myers EW, Lipman DJ. (1990) Basic local alignment search tool. *J Mol*
357 *Biol.* ; 215(3):403-10. [https://doi.org/10.1016/S0022-2836\(05\)80360-2](https://doi.org/10.1016/S0022-2836(05)80360-2)

358

359 Aury, JM, Engelen, S, Istance, B, Monat, C, Lasserre-Zuber, P, Belser, C, Cruaud, C, Rimbert, H,
360 Leroy, P, Arribat, S, Dufau, I, Bellec, A, Grimbichler, D, Papon, N, Paux, E, Ranoux, M, Alberti, A,
361 Wincker, P, Choulet, F (2022). Long-read and chromosome-scale assembly of the hexaploid wheat
362 genome achieves high resolution for research and breeding. *Gigascience*, 11.
363 <https://doi.org/10.1093/gigascience/giac034>

364 Belser, C, Istance, B, Denis, E, Dubarry, M, Baurens, FC, Falentin, C, Genete, M, Berrabah, W,
365 Chèvre, AM, Delourme, R, Deniot, G, Denoeud, F, Duffé, P, Engelen, S, Lemainque, A, Manzanares-
366 Dauleux, M, Martin, G, Morice, J, Noel, B, Vekemans, X, D'Hont, A, Rousseau-Gueutin, M, Barbe, V,
367 Cruaud, C, Wincker, P, Aury, JM (2018). Chromosome-scale assemblies of plant genomes using
368 nanopore long reads and optical maps. *Nat Plants*, 4, 11:879-887. <https://doi.org/10.1038/s41477-018-0289-4>

370 Belser, C, Baurens, FC, Noel, B, Martin, G, Cruaud, C, Istance, B, Yahiaoui, N, Labadie, K, Hřibová, E,
371 Doležel, J, Lemainque, A, Wincker, P, D'Hont, A, Aury, JM (2021). Telomere-to-telomere gapless
372 chromosomes of banana using nanopore sequencing. *Commun Biol*, 4, 1:1047.
373 <https://doi.org/10.1038/s42003-021-02559-3>

374 Cabanettes F, Klopp C. (2018) D-GENIES: dot plot large genomes in an interactive, efficient and
375 simple way. *PeerJ* 6:e4958. <https://doi.org/10.7717/peerj.4958>

376 Danecek, P, Bonfield, JK, Liddle, J, Marshall, J, Ohan, V, Pollard, MO, Whitwham, A, Keane, T,
377 McCarthy, SA, Davies, RM, Li, H (2021). Twelve years of SAMtools and BCFtools. *Gigascience*, 10,
378 2. <https://doi.org/10.1093/gigascience/giab008>

379 De Coster, W, D'Hert, S, Schultz, DT, Cruts, M, Van Broeckhoven, C (2018). NanoPack: visualizing
380 and processing long-read sequencing data. *Bioinformatics*, 34, 15:2666-2669.
381 <https://doi.org/10.1093/bioinformatics/bty149>

382 Flynn, JM, Hubley, R, Goubert, C, Rosen, J, Clark, AG, Feschotte, C, Smit, AF (2020).
383 RepeatModeler2 for automated genomic discovery of transposable element families. *Proc Natl Acad*
384 *Sci U S A*, 117, 17:9451-9457. <https://doi.org/10.1073/pnas.1921046117>

13

385 Guan, D, McCarthy, SA, Wood, J, Howe, K, Wang, Y, Durbin, R (2020). Identifying and removing
386 haplotypic duplication in primary genome assemblies. *Bioinformatics*, 36, 9:2896-2898.
387 <https://doi.org/10.1093/bioinformatics/btaa025>

388 Huang, K, Rieseberg, LH (2020). Frequency, Origins, and Evolutionary Role of Chromosomal
389 Inversions in Plants. *Front Plant Sci*, 11:296. <https://doi.org/10.3389/fpls.2020.00296>

390 Istance, B, Belser, C, Aury, JM (2020). BiSCoT: improving large eukaryotic genome assemblies with
391 optical maps. *PeerJ*, 8:e10150. <https://doi.org/10.1101/674721>

392

393 Istance, B, Belser, C, Falentin, C, Labadie, K, Boideau, F, Deniot, G, Maillet, L, Cruaud, C, Bertrand, L,
394 Chèvre, AM, Wincker, P, Rousseau-Gueutin, M, Aury, JM (2021). Sequencing and Chromosome-
395 Scale Assembly of Plant Genomes, *Brassica rapa* as a Use Case. *Biology (Basel)*, 10,732.
396 <https://doi.org/10.3390/biology10080732>

397

398 Kamm, A, Schmidt, T, Heslop-Harrison, JS (1994). Molecular and physical organization of highly
399 repetitive, undermethylated DNA from *Pennisetum glaucum*. *Mol Gen Genet*, 244, 4:420-5.
400 <https://doi.org/10.1007/BF00286694>

401

402 Kolmogorov, M, Yuan, J, Lin, Y, Pevzner, PA (2019). Assembly of long, error-prone reads using
403 repeat graphs. *Nat Biotechnol*, 37, 5:540-546, <https://doi.org/10.1038/s41587-019-0072-8>

404 Li H. and Durbin R. (2010) Fast and accurate long-read alignment with Burrows-Wheeler transform.
405 *Bioinformatics*, 26, 589-595, <https://doi.org/10.1093/bioinformatics/btp698>

406 Li H. (2018). Minimap2: pairwise alignment for nucleotide sequences. *Bioinformatics*, 34:3094-3100,
407 <https://doi.org/10.1093/bioinformatics/bty191>

408 Manni, M, Berkeley, MR, Seppey, M, Zdobnov, EM (2021). BUSCO: Assessing Genomic Data Quality
409 and Beyond. *Curr Protoc*, 1, 12:e323. <https://doi.org/10.1002/cpz1.323>

410 Mariac C, Zekraoui L and Leblanc O (2019). High molecular weight DNA extraction from plant nuclei
411 isolation. *protocols.io*. <https://dx.doi.org/10.17504/protocols.io.83shyne>

412 Martin M. (2011) Cutadapt removes adapter sequences from high-throughput sequencing reads.
413 *EMBnet.journal*, [S.I.], v. 17, n. 1, p. pp. 10-12. ISSN 2226-6089. <https://doi.org/10.14806/ej.17.1.200>

414 Medaka: Sequence correction provided by ONT Research. <https://github.com/nanoporetech/medaka>

415 Mengyang Xu, Lidong Guo, Shengqiang Gu, Ou Wang, Rui Zhang, Brock A Peters, Guangyi Fan, Xin
416 Liu, Xun Xu, Li Deng, Yongwei Zhang (2020) TGS-GapCloser: A fast and accurate gap closer for
417 large genomes with low coverage of error-prone long reads. *GigaScience*, Volume 9, Issue 9.
418 <https://doi.org/10.1093/gigascience/giaa094>

419

420 Orjuela J, Comte A, Ravel S, Charriat F, Vi T, Sabot F, Cunnac S (2022) CulebrONT: a streamlined
421 long reads multi-assembler pipeline for prokaryotic and eukaryotic genomes. Peer Community
422 Journal, Volume 2, article no. E46. <https://doi.org/10.24072/pcjournal.153>.

423 Roach, MJ, Schmidt, SA, Borneman, AR (2018). Purge Haplotts: allelic contig reassignment for third-
424 gen diploid genome assemblies. BMC Bioinformatics, 19, 1:460. [https://doi.org/10.1186/s12859-018-2485-7](https://doi.org/10.1186/s12859-018-
425 2485-7)

426 Shelton JM, Coleman MC, Herndon N, et al. (2015) Tools and pipelines for BioNano data: molecule
427 assembly pipeline and FASTA super scaffolding tool. BMC Genomics; 16:734.
428 <https://doi.org/10.1186/s12864-015-1911-8>

429 Shumate, A, Salzberg, SL (2020). Liftoff: accurate mapping of gene annotations. *Bioinformatics*, 37,
430 12:1639-43. <https://doi.org/10.1093/bioinformatics/btaa1016>

431 Tarailo-Graovac, M, Chen, N (2009). Using RepeatMasker to identify repetitive elements in genomic
432 sequences. Curr Protoc Bioinformatics, Chapter 4:Unit 4.10.
433 <https://doi.org/10.1002/0471250953.bi0410s25>

434 Varshney, RK, Shi, C, Thudi, M, Mariac, C, Wallace, J, Qi, P, Zhang, H, Zhao, Y, Wang, X, Rathore,
435 A, Srivastava, RK, Chitikineni, A, Fan, G, Bajaj, P, Punnuri, S, Gupta, SK, Wang, H, Jiang, Y,
436 Couderc, M, Katta, MAVSK, Paudel, DR, Mungra, KD, Chen, W, Harris-Shultz, KR, Garg, V, Desai, N,
437 Doddamani, D, Kane, NA, Conner, JA, Ghatak, A, Chaturvedi, P, Subramaniam, S, Yadav, OP,
438 Berthouly-Salazar, C, Hamidou, F, Wang, J, Liang, X, Clotault, J, Upadhyaya, HD, Cubry, P, Rhoné,
439 B, Gueye, MC, Sunkar, R, Dupuy, C, Sparvoli, F, Cheng, S, Mahala, RS, Singh, B, Yadav, RS, Lyons,
440 E, Datta, SK, Hash, CT, Devos, KM, Buckler, E, Bennetzen, JL, Paterson, AH, Ozias-Akins, P,
441 Grando, S, Wang, J, Mohapatra, T, Weckwerth, W, Reif, JC, Liu, X, Vigouroux, Y, Xu, X (2017). Pearl
442 millet genome sequence provides a resource to improve agronomic traits in arid environments. Nat
443 Biotechnol, 35, 10:969-976. <http://dx.doi.org/10.1038/nbt.3943>

444 Vaser R, Sović I, Nagarajan N, Šikić M. (2017) Fast and accurate de novo genome assembly from
445 long uncorrected reads. Genome Res. 27(5):737-746. <https://doi: 10.1101/gr.214270.116>.

446 Vasimuddin M, Misra S, Li H and Aluru S, (2019) Efficient Architecture-Aware Acceleration of BWA-
447 MEM for Multicore Systems, IEEE International Parallel and Distributed Processing Symposium
448 (IPDPS) pp. 314-324, <https://doi.org/10.1109/IPDPS.2019.00041>

449 Yuan, Y, Chung, CY, Chan, TF (2020). Advances in optical mapping for genomic research. *Comput
450 Struct Biotechnol J*, 18:2051-2062. <https://doi.org/10.1016/j.csbj.2020.07.018>

451 Wellenreuther M, Bernatchez L. (2018) Eco-Evolutionary Genomics of Chromosomal Inversions.
452 Trends Ecol Evol., 33(6):427-440. <https://doi.org/10.1016/j.tree.2018.04.002>

453 Wickham H (2016). *ggplot2: Elegant Graphics for Data Analysis*. Springer-Verlag New York. ISBN
454 978-3-319-24277-4. <http://ggplot2.org>

15

455 **Figure 1** Alignments between the chromosomes of the new assembly and the chromosomes of the
456 Tift 23D2B1-P1-P5 reference genome.

457 Plots of the alignments obtained with D-genies are shown between the old reference genome on the
458 horizontal axis, and the new assembly on the vertical axis. Alignments with identities between 50 and
459 75% are in light green, and in dark green are alignments with identities between 75 and 100%.
460 Orange rectangles on the vertical axis correspond to the positions of the centromeric satellite
461 sequence on each chromosome of the new assembly. A large region of ~ 100 Mb is missing on the
462 chromosome 7 of the reference genome represented on the horizontal axis.

463

464 **Figure S1** Pipeline of the genome assembly combining long reads and optical mapping.

465 Assembly of the ONT long reads was performed with the assembler Flye. Two rounds of Racon and
466 Medaka were used to polish and correct the ONT contigs using the long reads. The ONT contigs were
467 polished with high quality Illumina short reads using Hapo-G. *De novo* assembly of the Bionano
468 molecules was performed using Bionano Solve pipeline. Hybrid scaffolding of the ONT contigs was
469 performed using the Bionano assembled optical maps with Bionano Solve. ONT contigs not aligned to
470 an optical map were placed in the chrUN. We used BiSCoT in order to remove artefactual duplications
471 from the hybrid scaffolds. TGS Gap-Closer was used to perform gap filling and reduce the total
472 number of Ns in the hybrid scaffolds. A last step of high quality short reads correction with Hapo-G
473 was performed. Chromosomes were finally builded using RagTag and the pearl millet Tift 23D2B1-P1-
474 P5 reference genome (Varshney et al. 2017) as a guide. Manual curations were performed based on
475 RagTag confidence scores and hybrid scaffolds with grouping confidence scores below 0.7 were
476 added to the chrUN.

477

478 **Figure S2** Correlation between the chromosome size estimated using optical maps and the
479 chromosome lengths of the reference.

480 The correlation is marginally significant (Pearson correlation coefficient $r=0.736$, $p\text{-value}=0.059$). The
481 size of chromosome 7 appeared underestimated by roughly 128 Mb.

482

483 **Figure S3** Comparison between the Tift 23D2B1-P1-P5 pearl millet reference genome and optical
484 maps

485 We show optical map alignments to each chromosome of the reference using Bionano Access. Dark
486 blue color corresponds to regions where labels are aligned between the optical maps and the
487 reference, and gray lines join the aligned labels between them. Yellow color represents regions
488 without label matches. Several cases of crossing lines between the reference genome and the optical
489 maps are shown. This pattern suggests discontinuity between the order of the contigs and scaffolds in
490 the assembly and the optical maps.

16

491 **Figure S4** Read depth histogram obtained with Purge Haplotype

492 The histogram represents the total number of bases of the assemblies (on the vertical axis) with a
493 given read-depth (on the horizontal axis). No evidence of duplication is shown in the plot. The pic at a
494 read-depth equal to 0 corresponds to Ns regions between ONT contigs positioned on the hybrid
495 scaffolds.

496

497 **Figure S5** Comparison of the alignments between the PMiGAP257/IP-4927 optical maps and the
498 chromosomes of both the old and the new assembly

499 Optical maps from the PMiGAP257/IP-4927 line were aligned to both the new and previous genomes
500 with Bionano Solve. Dark blue color corresponds to regions where labels are aligned between the
501 optical maps and the genomes, and gray lines join the aligned labels between them. Yellow color
502 represents regions without label matches. Overall, the new genome showed less crossing lines with
503 the optical maps of PMiGAP257/IP-4927 line, a signature of better continuity of the order of the
504 contigs and scaffolds in the new assembly.

Figure 1

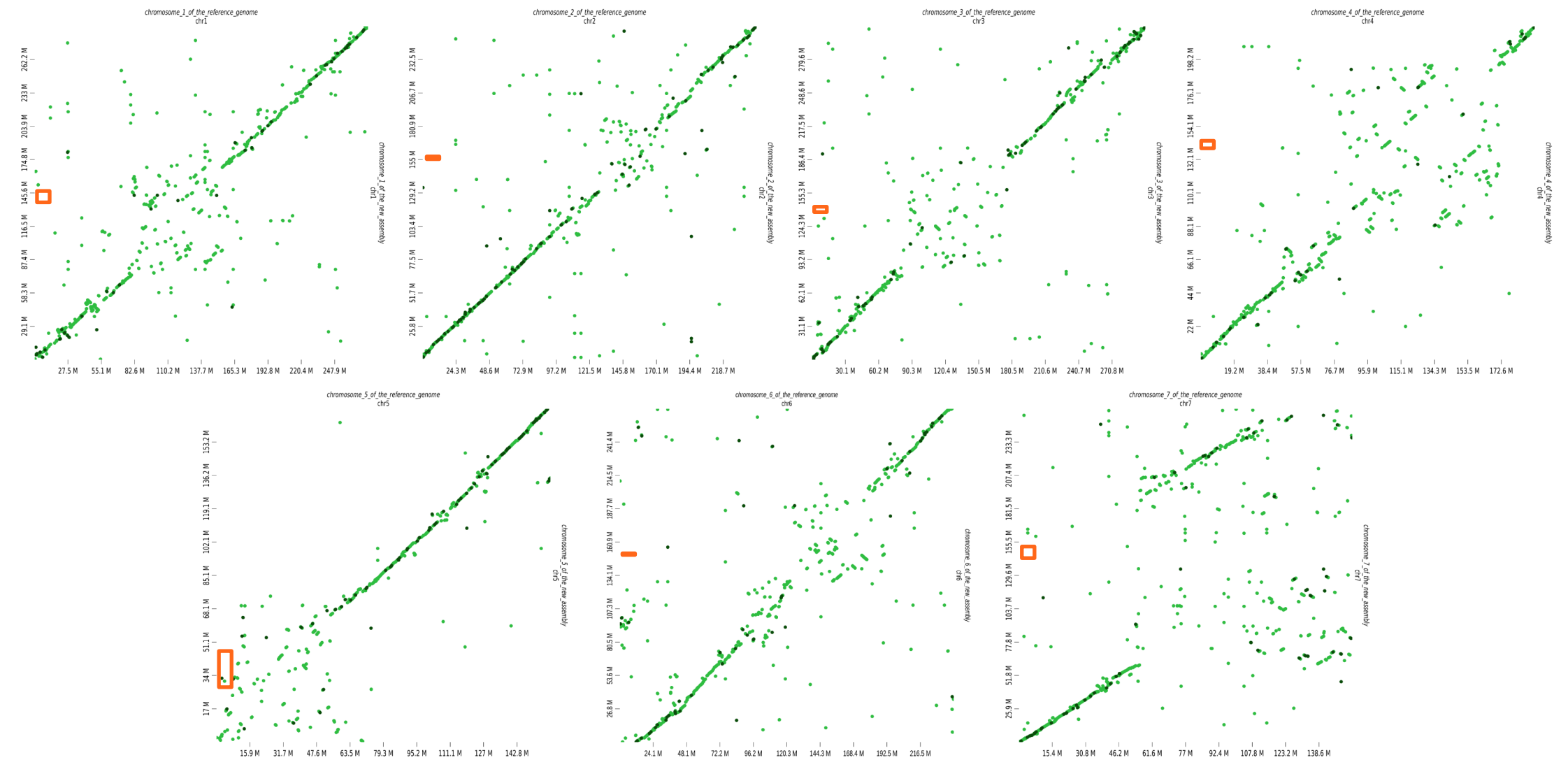


Table 1 Statistics of the pearl millet Tift 23D2B1-P1-P5 reference genome and of the new assembly

	Reference assembly	New assembly
Total assembly		
Total length	1.82 Gb	1.85 Gb
GC content	47.9 %	49.5 %
Complete BUSCOs	95.4% (of 956 genes)	98.4% (of 4896 genes)
Chromosomes		
Number of chr	7	7
Total length of chr	1,564,537,551 bp	1,778,181,882 bp
Percentage of Ns	13.5%	0.3%
Scaffolds		
Number of scaffolds	25,241	72
Longest scaffold	4,816,714 bp	167,249,600 bp
N50 (scaffolds)	884,945 bp	85,795,566 bp
Contigs		
Number of contigs	175,708	3,641
Longest contig	282,901 bp	6,842,273 bp
N50 (contigs)	18,180 bp	1,209,791 bp

Statistics were calculated for the new assembly and compared to the statistics of the previous Tift 23D2B1-P1-P5 published genome assembly (Varshney et al. 2017). The gene completeness of the new assembly was estimated with BUSCO (v. 5.4.3, Manni et al. 2021) and the Poales dataset (odb10) composed of 4896 genes. Complete BUSCO percentage of the reference genome is the one previously published with a smaller database of 956 genes (Varshney et al. 2017).

Figure S1

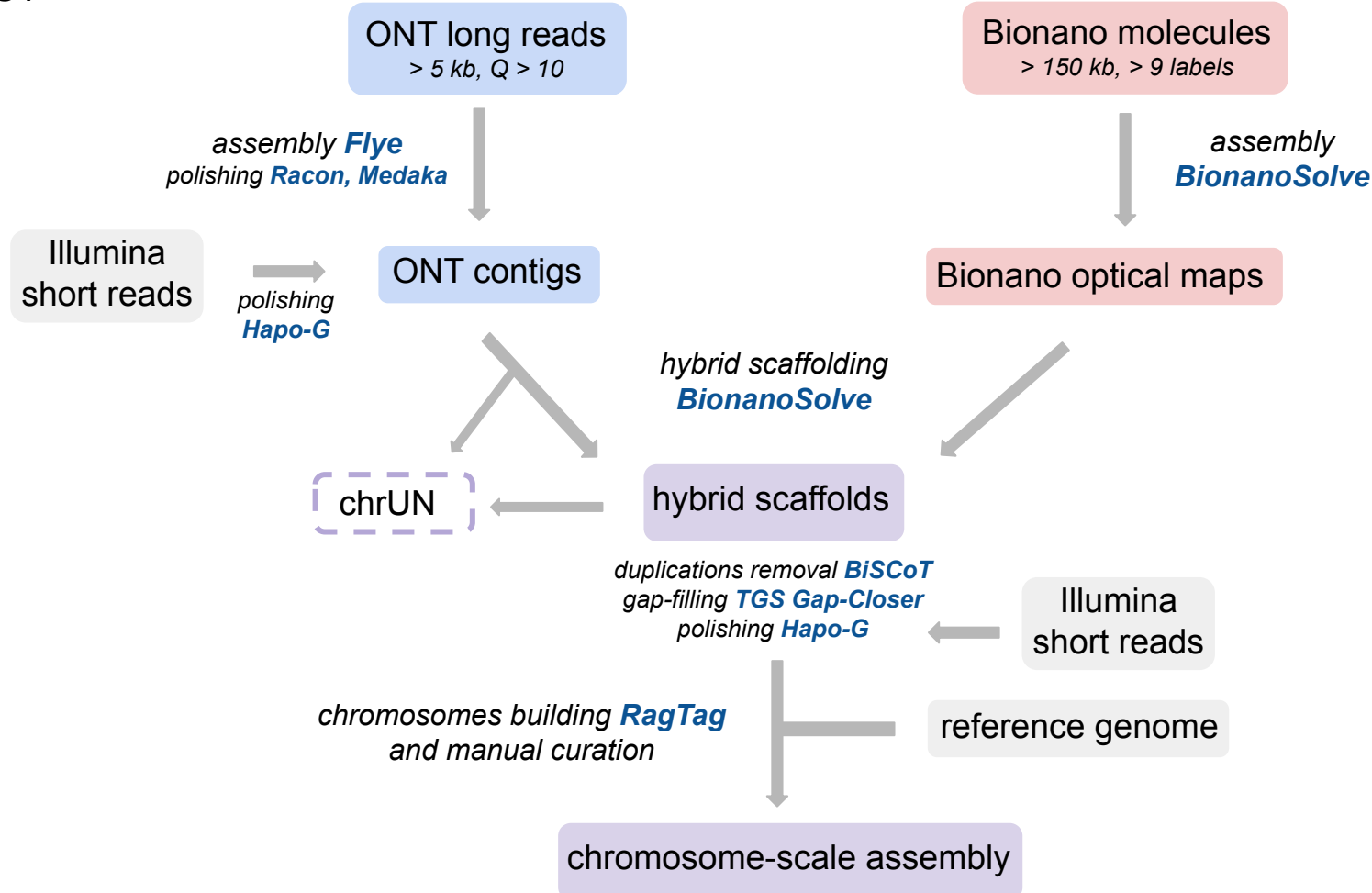


Figure S2

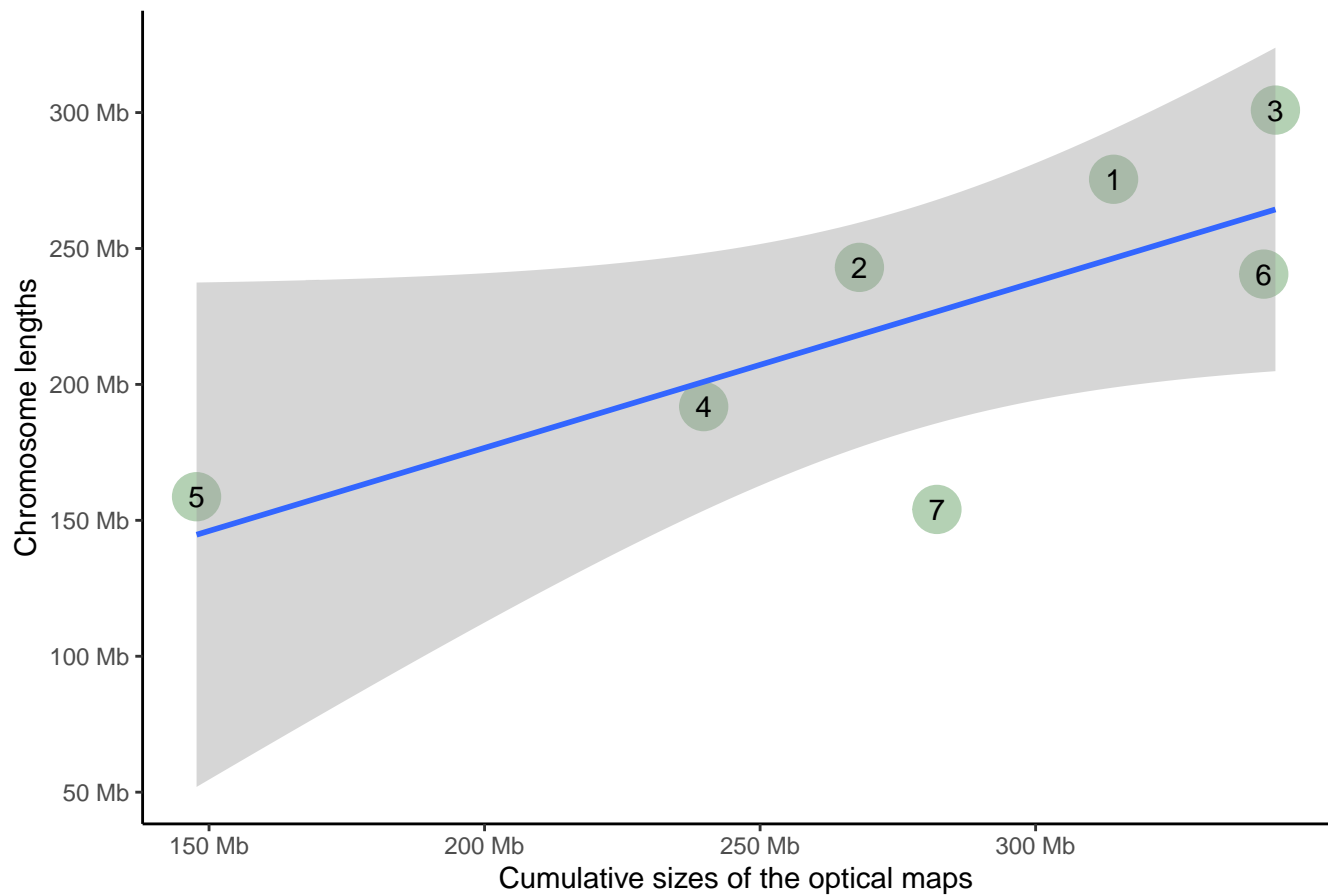
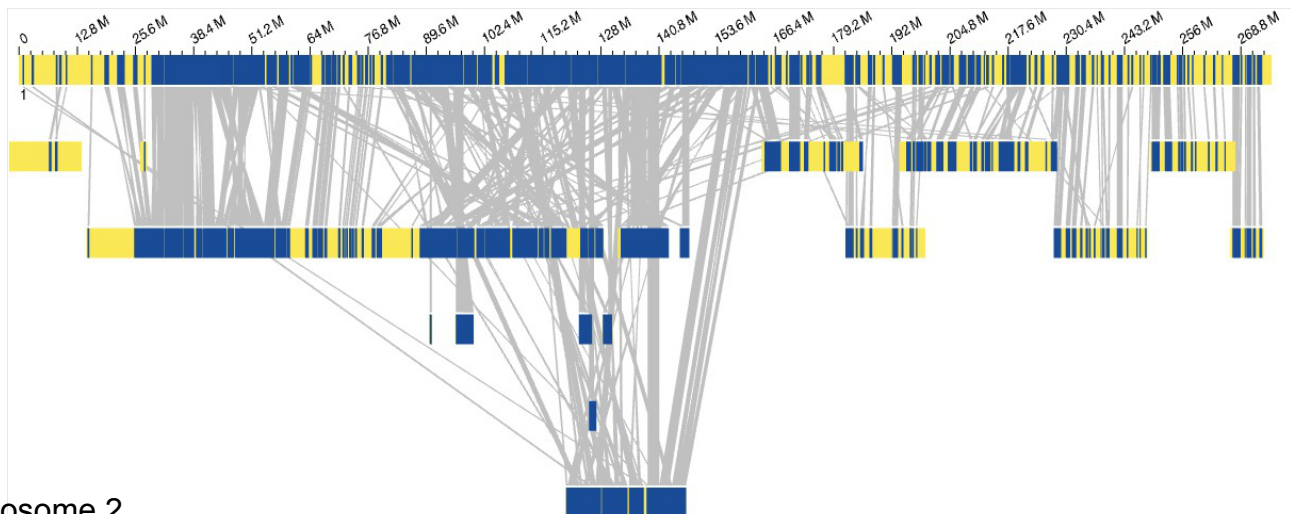
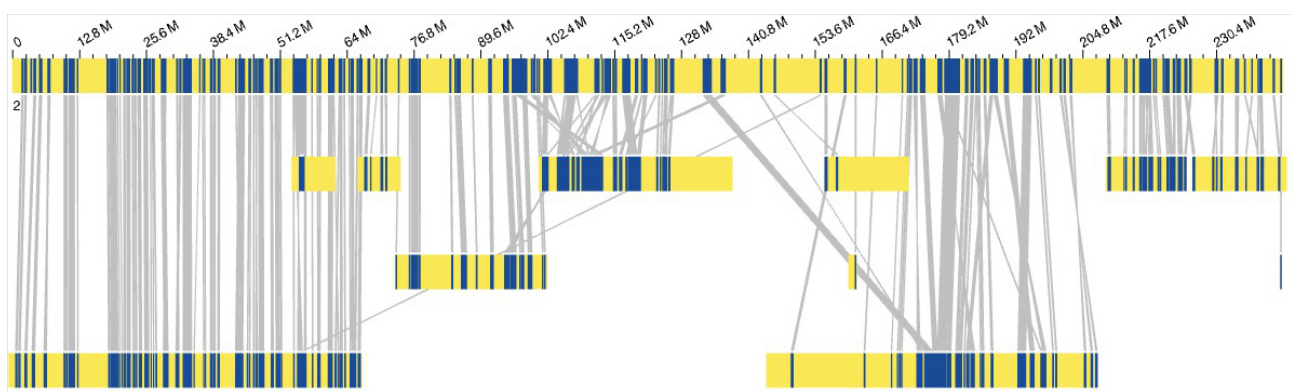


Figure S3 (to be continued)

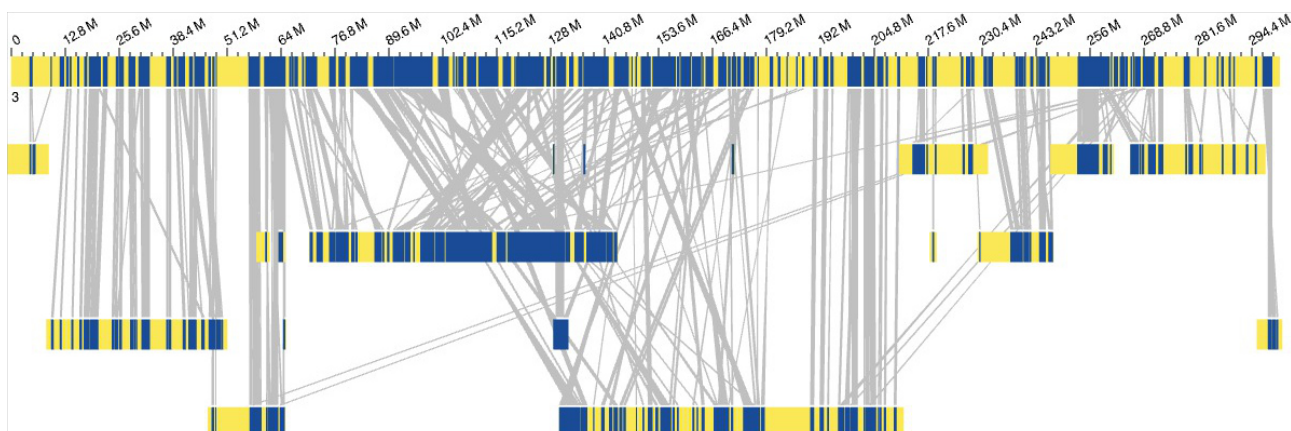
Chromosome 1



Chromosome 2



Chromosome 3



Chromosome 4

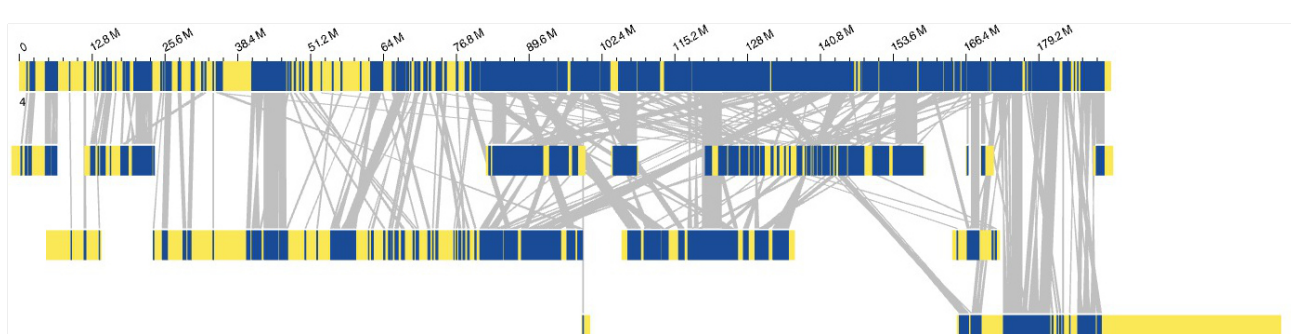
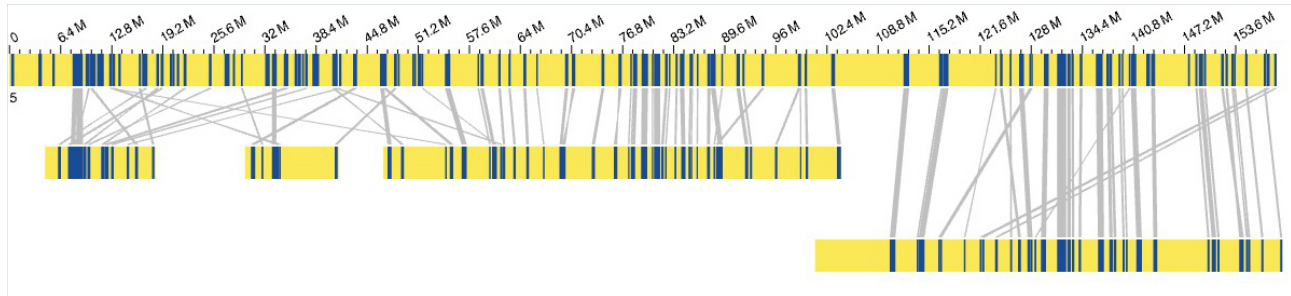
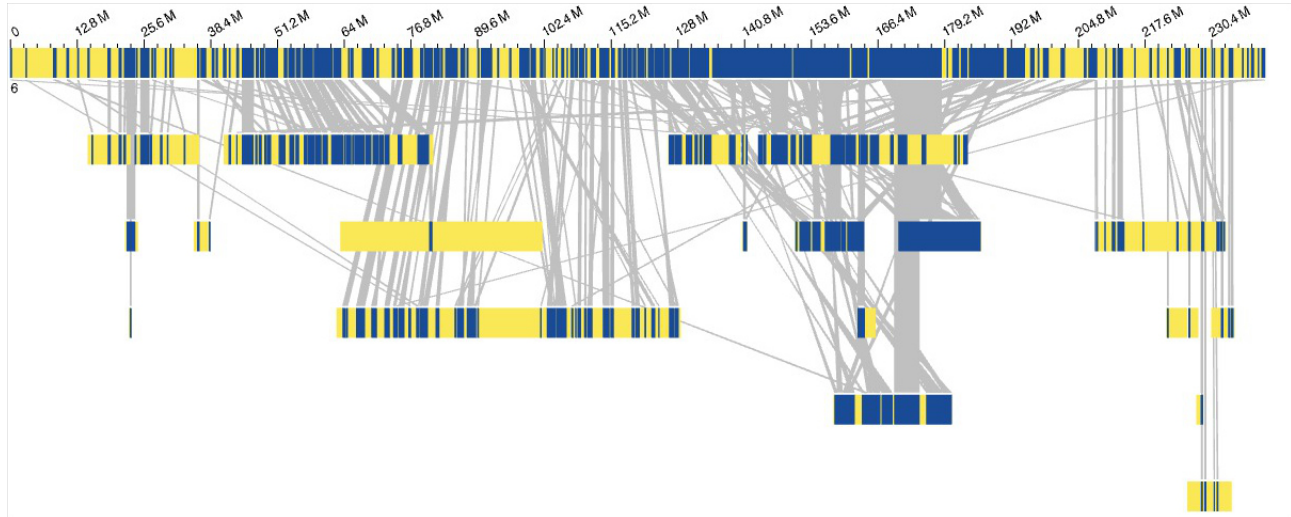


Figure S3 (continued)

Chromosome 5



Chromosome 6



Chromosome 7

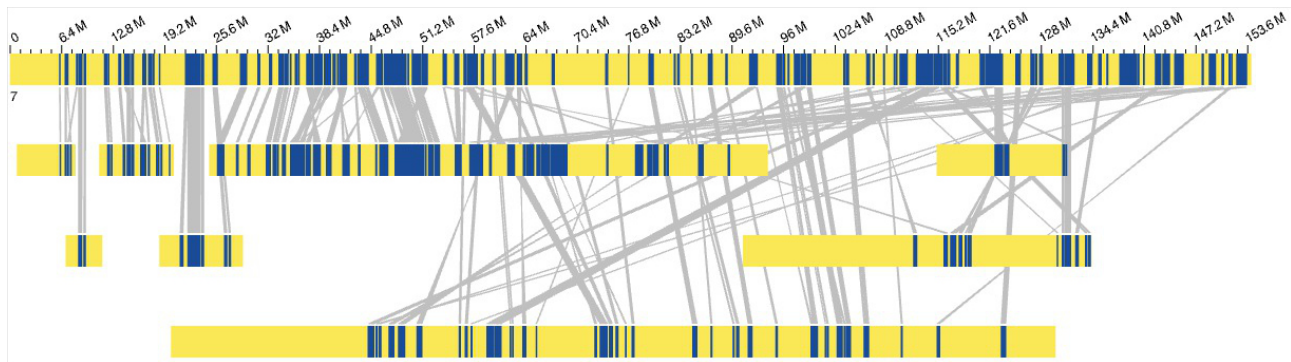
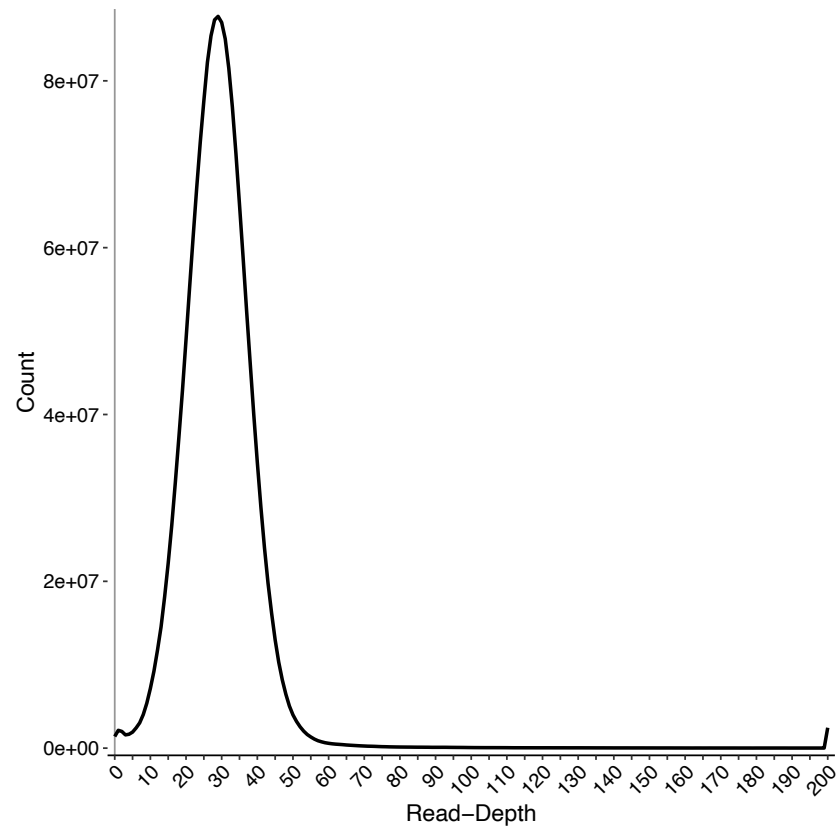


Figure S4

A



B

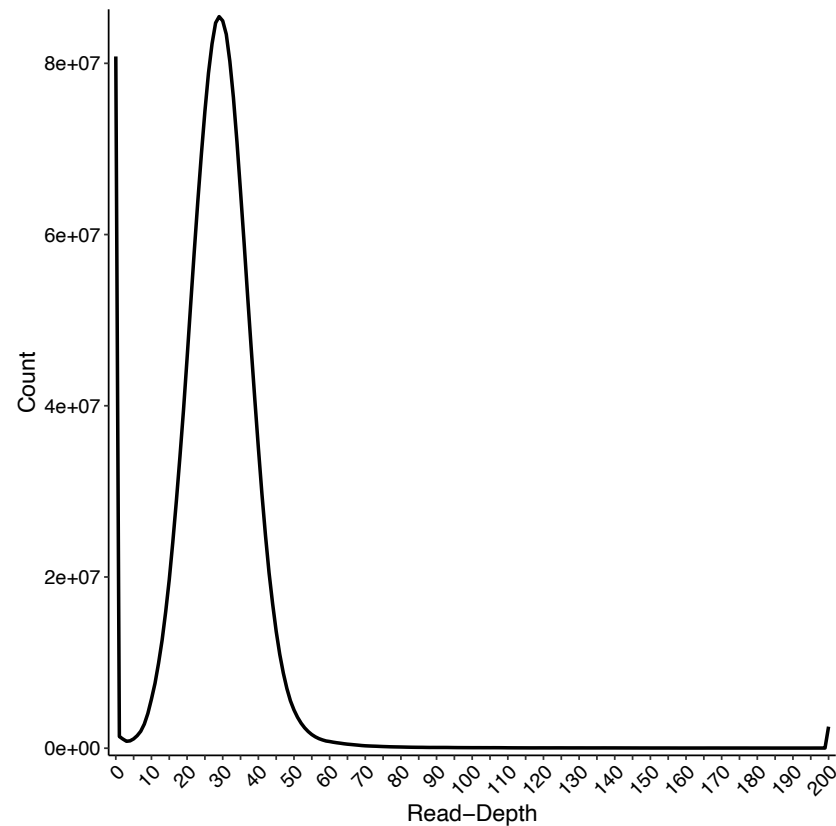
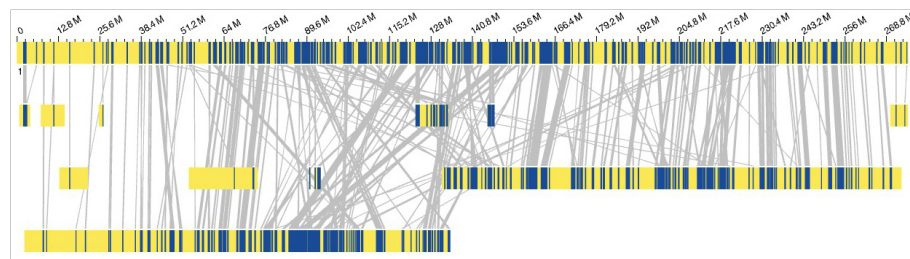
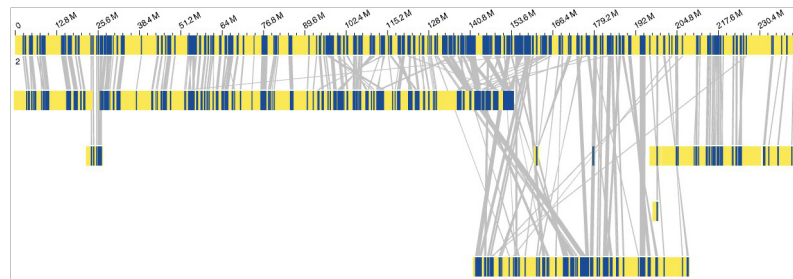


Figure S5 (to be continued)

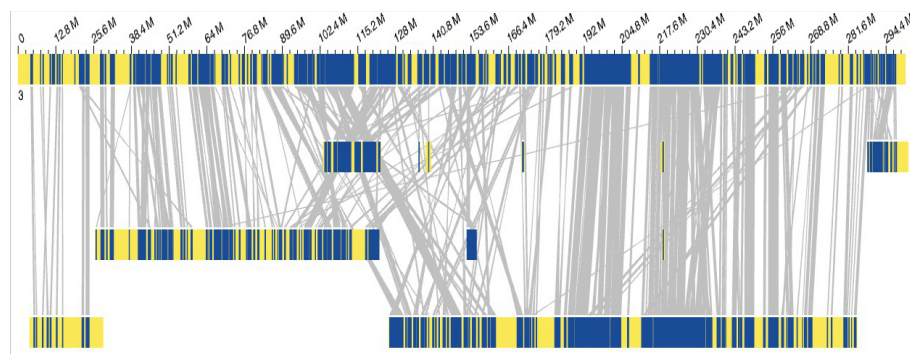
chromosome 1



chromosome 2



chromosome 3



chromosome 4

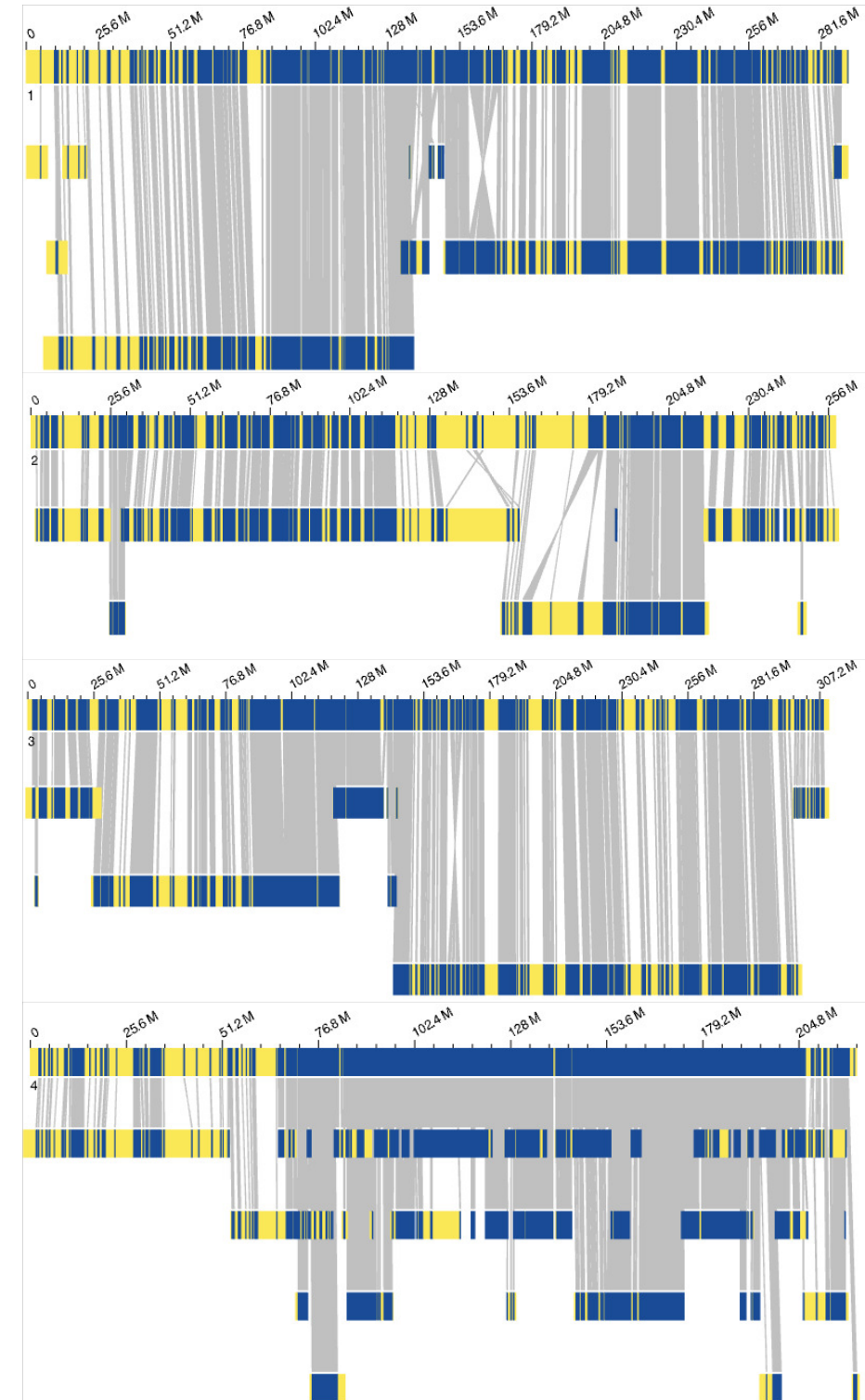
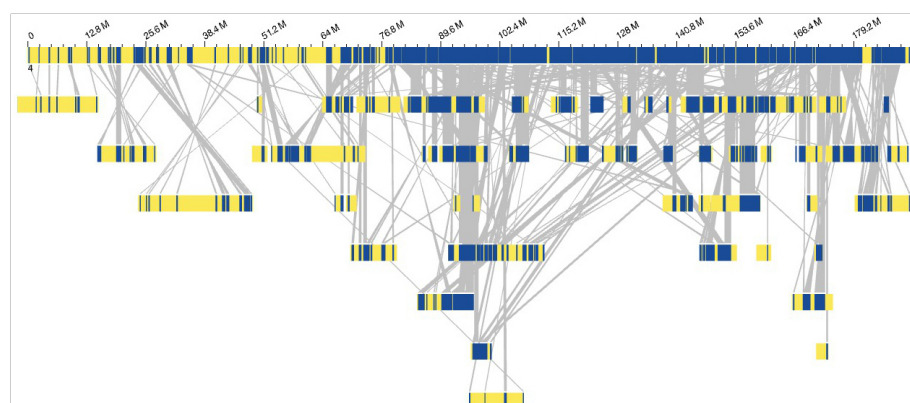
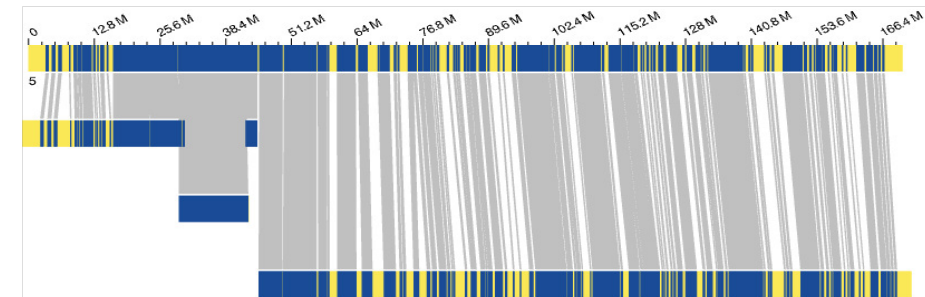
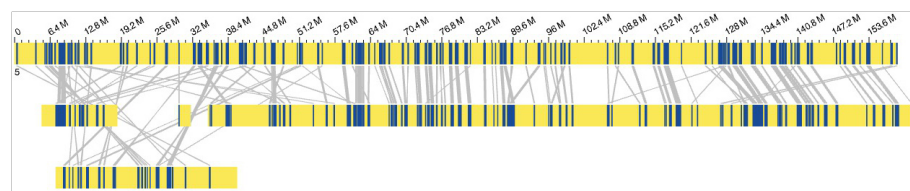
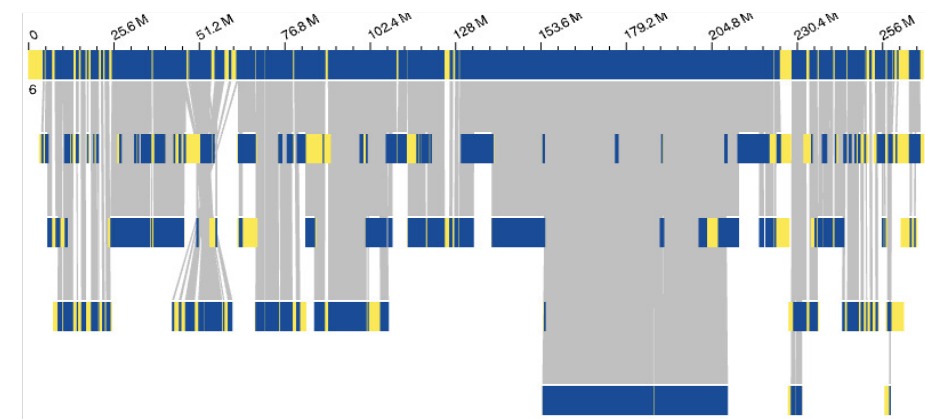
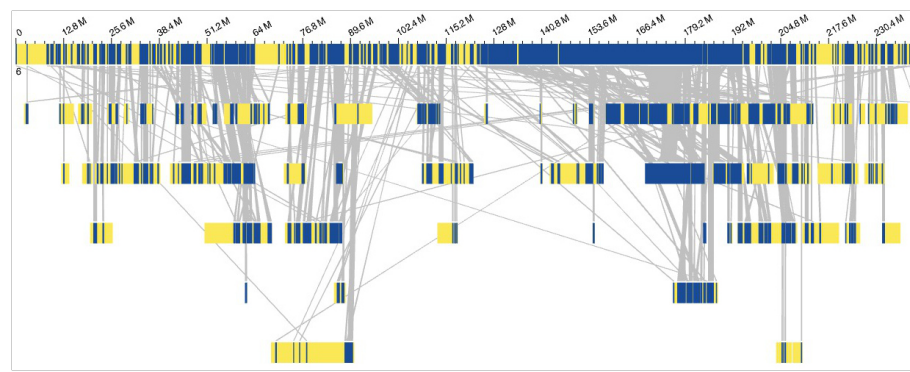


Figure S5 (continued)

chromosome 5



chromosome 6



chromosome 7

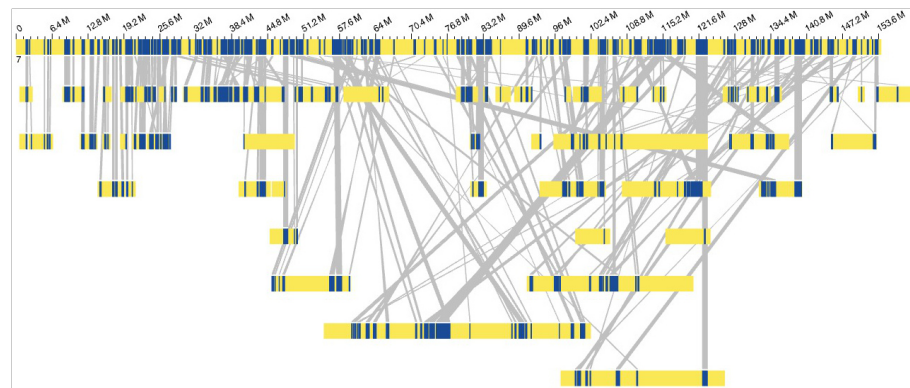


Table S1 (to be continued) Grouping, location and orientation confidence scores obtained with RagTag and assignation of the scaffolds to chromosomes 1, 2 and 3

scaffolds	positions	Length (Mb)	Grouping confidence	Location confidence	Orientatin confidence	Assignation	Orientation	Manual curation	Commentary
Scaffold_100110	1	0.23	1.00	1.00	1.00	chr1	+		
Scaffold_100122	226189	0.24	0.89	0.01	1.00	chr1	-		
Scaffold_334	466543	0.38	0.57	0.00	0.48	chrUN			
Scaffold_1755	848567	0.28	0.36	1.00	1.00	chrUN			
Scaffold_684	1125736	135.22	0.89	0.43	0.67	chr1	+		
Scaffold_100099	136349156	0.34	0.82	0.00	1.00	chr1	-		
Scaffold_3432	136691461	3.88	0.99	0.76	0.84	chr1	+		
Scaffold_100068	140568769	2.74	0.97	0.10	0.75	chr1	+	reversed	Optical maps alignments
Scaffold_100077	143312877	1.21	0.98	0.01	0.80	chr1	-		
Scaffold_1194	144525903	1.97	0.95	0.03	0.74	chr1	+		
Scaffold_100074	146495435	1.95	1.00	0.03	0.70	chr1	+		
Scaffold_605	148447732	63.83	0.93	0.22	0.67	chr1	-		
Scaffold_2678	212275389	0.37	0.51	0.00	0.62	chrUN			
Scaffold_1750	212649219	70.59	0.90	0.23	0.85	chr1	+		
Scaffold_100120	283239647	0.25	0.50	1.00	1.00	chrUN	+		
Scaffold_653	283486746	0.47	0.52	1.00	1.00	chrUN	+		
Scaffold_1948	283960203	8.73	0.97	0.03	0.89	chr1	+		
Scaffold_2542	292688886	0.36	1.00	1.00	1.00	chr1	+		
Scaffold_2622	1	139.50	0.91	0.52	0.87	chr2	-		
Scaffold_100115	139503085	0.33	0.66	0.00	1.00	chrUN	+		
Scaffold_100390	139831199	0.10	0.37	0.00	0.96	chrUN	+		
Scaffold_588	139935275	0.19	0.95	1.00	1.00	chr2	+		
Scaffold_100035	140122483	15.16	0.72	0.05	0.62	chr2	-		
Scaffold_100078	155280469	1.39	0.54	0.01	0.49	chrUN			
Scaffold_34	156672757	85.80	0.87	0.31	0.78	chr2	-		
Scaffold_3074	242468423	17.38	0.83	0.06	0.90	chr2	+		
Scaffold_2923	259847680	0.34	0.31	0.00	1.00	chrUN			
Scaffold_1820	260183567	0.36	1.00	1.00	1.00	chr2	+		
Scaffold_100046	1	9.37	0.91	0.03	0.75	chr3	-		
Scaffold_405	9365327	41.21	0.89	0.12	0.81	chr3	-		
Scaffold_100109	50572670	0.26	0.26	0.00	0.75	chrUN			
Scaffold_1980	50830930	88.32	0.91	0.28	0.41	chr3	-	reversed	Reference and optical maps alignments and centromeric repeats at the beginning of the scaffold_1980
Scaffold_3136	139153606	0.47	0.96	0.00	0.86	chr3	+		Centromeric repeats at the beginning of the scaffold_3136
Scaffold_2854	139623671	3.56	0.98	0.02	0.49	chr3	+		
Scaffold_339	143188428	0.64	0.46	0.00	0.90	chrUN	+		
Scaffold_1791	143833524	2.10	0.25	0.00	0.83	chrUN	+		
Scaffold_100089	145932556	0.52	1.00	1.00	1.00	chr3	-		
Scaffold_391	146447927	167.25	0.92	0.50	0.72	chr3	+		

Tables S1 (continued) Grouping, location and orientation confidence scores obtained with RagTag and assignation of the scaffolds to chromosomes 4, 5, 6 and 7

Scaffolds	Positions	Length (Mb)	Grouping confidence	Location confidence	Orientation confidence	Assignation	Orientation	Manual curation	Commentary
Scaffold_1420	1	28.28	0.85	0.12	0.72	chr4	-		
Scaffold_503	28276606	111.45	0.83	0.49	0.62	chr4	-		
Scaffold_100088	139728581	0.39	0.46	0.00	1.00	chrUN	+		
Scaffold_100123	140116163	0.21	0.80	1.00	1.00	chr4	+		
Scaffold_2012	140326476	4.57	0.96	0.05	0.90	chr4	+		
Scaffold_100021	144893014	29.45	0.80	0.14	0.53	chr4	+		
Scaffold_100032	174339204	17.11	0.80	0.09	0.54	chr4	-		
Scaffold_100106	191448136	0.28	1.00	1.00	1.00	chr4	+		
Scaffold_100051	191725424	7.79	0.52	0.02	0.84	chrUN	+		
Scaffold_1644	199517487	2.03	0.48	0.01	1.00	chrUN	+		
Scaffold_8135	201546798	25.84	0.78	0.11	0.65	chr4	-	split	Scaffold_8135 aligned both to the chr4 and chr5
frag2_42-68Mb									
Scaffold_100063	227389902	3.00	0.89	0.02	0.96	chr4	+		
Scaffold_8135	1	42.33	0.87	0.24	0.54	chr5	-	split	Scaffold_8135 aligned both to chr4 and chr5
frag1_1-42Mb									
Scaffold_3415	42330101	2.32	1.00	0.03	0.99	chr5	-		
Scaffold_264	44645588	68.28	0.83	0.36	0.84	chr5	-		
Scaffold_1218	112928476	57.28	0.91	0.33	0.93	chr5	+		
Scaffold_100128	1	0.18	1.00	1.00	1.00	chr6	+		
Scaffold_293	177348	9.87	0.95	0.04	0.94	chr6	-		
Scaffold_1452	10044232	52.10	0.91	0.20	0.88	chr6	-		
Scaffold_100172	62141462	12.94	0.74	0.04	0.67	chr6	-	Moved between Scaffold_100025 and 4533	Optical maps alignments
Scaffold_4533	75082935	0.66	0.75	0.01	0.66	chr6	-	Moved between Scaffold_100172 and 184	Optical maps alignments
Scaffold_100086	75740204	0.95	0.95	0.04	0.59	chr6	-	Moved between Scaffold_100036 and 100025	Optical maps alignments and centromeric repeats all along the Scaffold_100086
Scaffold_852	76689220	76.74	0.86	0.28	0.66	chr6	+	Moved between Scaffold_1452 and 100036	
Scaffold_100025	153429261	21.67	0.89	0.09	0.42	chr6	-	Moved between Scaffold_100086 and 100172	Centromeric repeats at the beginning of the Scaffold_100025
Scaffold_100036	175096010	15.31	0.95	0.18	0.50	chr6	+	Moved between Scaffold_852 and 100086	Centromeric repeats at the end of the Scaffold_100036
Scaffold_184	190410105	67.00	0.84	0.23	0.81	chr6	-		
Scaffold_3195	257410051	5.55	0.91	0.03	0.95	chr6	-		
Scaffold_1763	262955763	5.22	0.88	0.08	0.90	chr6	-		
Scaffold_100102	1	0.29	0.99	0.36	0.63	chr7	+		
Scaffold_100055	292087	6.80	0.96	0.07	0.94	chr7	+		
Scaffold_1301	7091952	146.59	0.58	0.51	0.71	chr7	-		
Scaffold_2567	153684823	105.08	0.61	0.40	0.70	chr7	+		
Scaffold_100092	258763135	0.10	1.00	1.00	1.00	chr7	-		
Scaffold_3516	258865757	0.38	1.00	1.00	1.00	chr7	-		
Scaffold_100127	259248350	0.23	0.62	0.00	1.00	chrUN	+		

Table S2 Positions of the centromeric specific sequence on the chromosomes of the new assembly

	Positions of alignments	Number of alignments
chr1	134.1 - 147.8 Mb	93/93 (100%)
chr2	154.9 - 156.9 Mb	47/54 (87%)
chr3	138.8 - 143.7 Mb	1981/1981 (100%)
chr4	139.5 - 144.4 Mb	57/57 (100%)
chr5	29.2 - 44.9 Mb	208/208 (100%)
chr6	154.0 - 155.2 Mb	410/411 (99%)
chr7	144.2 - 153.9 Mb	102/102 (100%)

The 137 bp centromere specific sequence (Kamm et al. 1994) was aligned to each chromosome of the new assembly using blast (v. 2.9.0+, Altschul et al 1990). We only kept alignments longer than 100 bases and with an identity higher than 80%. Each line of the table has to be read as follows: for chromosome 1, 100% of the filtered alignments were found between 134.1 and 147.8 Mb.